

RESEARCH AND EDUCATION

Accuracy of a complete arch noncalibrated splinting implant scanning technique with a palatal orientation recorded by using different intraoral scanners

Marta Revilla-León, DDS, MSD, PhD,^a Rocio Cascos, DDS, MSD,^b Abdul B. Barmak, MD, MSc, EdD,^c John C. Kois, DMD, MSD,^d and Miguel Gómez-Polo, DDS, PhD^e

ABSTRACT

Statement of problem. The accuracy of noncalibrated splinting implant scanning techniques that include horizontal implant scan bodies (ISBs) positioned connecting the implants by following the shape of the dental arch have previously been analyzed. A novel horizontal ISB connected in the center of the arch has been introduced; however, the accuracy of this noncalibrated splinting implant scanning technique with a palatal orientation is unknown.

Purpose. The purpose of this in vitro study was to compare the accuracy of a nonsplinting and noncalibrated splinting implant scanning technique recorded using 5 intraoral scanners (IOSs).

Material and methods. A laboratory scan (reference scan) of an edentulous stone cast with 6 implant abutment analogs (MultiUnit Abutment Plus Replica) was acquired (T710). Five groups were created based on the IOS tested: TRIOS5, Primescan, i700, Aoralscan3, and iTero Element 5D. Two subgroups were defined based on the implant scanning technique used to record complete arch implant scans: a nonsplinted (NS-ISB subgroup) or noncalibrated splinting (NCS-IOC group) implant scanning technique (n=10). In the NS-ISB subgroup, an ISB (TrueScan Body) was positioned on each implant abutment, and complete arch implant scans were recorded and exported in standard tessellation language (STL) format. In the NCS-IOC subgroup, a horizontal ISB (IOConnect) was positioned on each implant abutment connecting them in the center of the palate. Implant scans were recorded, capturing only the section of the horizontal ISBs located in the center of the arch. Then, the scans were processed by a specific program (TruSuite), and the STL of the scans were exported. A program (Geomagic) was used to perform linear and angular measurements among the ISBs in the control scan and each specimen. The measurements obtained in the control scan were used as a reference to measure the scanning distortion of each specimen. The 2-way ANOVA Welch and pairwise multiple comparison Tukey tests were used to analyze trueness ($\alpha=.05$). The Levene and pairwise multiple comparison Wilcoxon rank tests were used to analyze precision ($\alpha=.05$).

Results. Linear trueness discrepancies were found among the groups ($P<.001$) and subgroups ($P<.001$), with a significant interaction group \times subgroup ($P=.002$). The NCS-IOC group had significantly better linear trueness than the NS-ISB group. The TRIOS5, Primescan, and Aoralscan3 systems had significantly better linear trueness than the i700 device. The Levene test revealed that the NCS-IOC group had significantly better linear precision than the NS-ISB group. Additionally, angular trueness discrepancies were revealed among the groups ($P<.001$) and subgroups ($P<.001$), with a significant interaction group \times subgroup ($P<.001$). The NCS-IOC group had significantly better angular trueness than the NS-ISB group. The i700 and Aoralscan3 systems had the best angular trueness. Additionally, the NCS-IOC group had significantly better angular precision than the NS-ISB group. The TRIOS5 and Aoralscan3 had the best angular precision.

Conclusions. The implant scanning technique used and IOS selected impacted the trueness and precision of complete arch implant scans. (J Prosthet Dent xxxx;xxx:xxx-xxx)

The authors declare that they have no known competing financial interests or personal relationships that could have appeared to influence the work reported in this paper. Funding This research did not receive any specific grant from funding agencies in the public, commercial, or not-for-profit sectors.

^aAffiliate Assistant Professor, Graduate Prosthodontics, Department of Restorative Dentistry, School of Dentistry, University of Washington, Seattle, Wash.; Faculty and Director, Research and Digital Dentistry, Kois Center, Seattle, Wash.; and Adjunct Professor, Department of Prosthodontics, School of Dental Medicine, Tufts University, Boston, Mass.

^bCollaborating Professor of Postgraduate Specialist in Advanced in Implant-Prosthodontics, Department of Conservative Dentistry and Prosthodontics, School of Dentistry, Complutense University of Madrid (UCM), Madrid, Spain; and Assistant Professor, Department of Prosthetic Dentistry, School of Dentistry, European University of Madrid, Madrid, Spain.

^cAssistant Professor Clinical Research and Biostatistics, Eastman Institute of Oral Health, University of Rochester Medical Center, Rochester, NY.

^dDirector, Kois Center, Seattle, Wash.; Affiliate Professor, Graduate in Prosthodontics, Department of Restorative Dentistry, School of Dentistry, University of Washington, Seattle, Wash.; and Private practice, Seattle, Wash.

^eAssociate Professor, Department of Conservative Dentistry and Prosthodontics, School of Dentistry, Complutense University of Madrid (UCM), Madrid, Spain.

Clinical Implications

The complete arch noncalibrated splinting implant scanning technique with a palatal orientation may provide a reliable implant scanning technique for acquiring a virtual definitive implant cast.

Different implant scanning techniques have been described for recording the 3-dimensional implant positions using intraoral scanners (IOSs), namely nonsplinting, noncalibrated splinting, calibrated implant scan bodies (ISBs), calibrated framework, and reverse impression methods.¹ The accuracy of these implant scanning techniques has been analyzed, with a mean scanning trueness ranging from 25 to 303 μm and a mean scanning precision from 8 to 181 μm .^{1–15} This accuracy variability has been related to the implant scanning technique used^{1–15} and also to other factors such as implant position,^{16–19} interimplant distance,^{20,21} and implant scan body (ISB) design or orientation.^{22–24} Additionally, the accuracy of IOSs can be impacted by different operator- and patient-related factors.^{25–27} Therefore, the operator recording an intraoral scan should understand and control these operator- and patient-related factors as much as possible, aiming to maximize the accuracy and efficiency of the IOS used.^{25–27}

Nonsplinting techniques involve recording implant scans without connecting the ISBs, while noncalibrated splinting implant scanning methods include connecting the ISBs before recording the intraoral digital scans.^{1,12} Among the noncalibrated splinting techniques, multiple devices or horizontal scan bodies have been described for connecting the ISBs.^{1,12} In the noncalibrated splinting procedures, the dimensions of the horizontal ISB have not been identified; therefore, only the theoretical or virtual dimensions of the horizontal ISB before its manufacturing are known.¹ The purpose of these horizontal ISBs is to connect adjacent implants; therefore, the position of ISBs follows the shape of the dental arch being scanned. A new design of horizontal ISBs has been developed aiming to improve the accuracy and facilitate the scanning procedure. These novel horizontal ISBs are placed so that they are connected in the center of the arch. However, the accuracy of these novel horizontal ISBs remains unknown.

The purpose of this *in vitro* study was to compare the accuracy (trueness and precision) of a nonsplinting and a noncalibrated splinting (IOConnect; TruAbutment) implant scanning technique recorded by using 5 IOSs (TRIOS 5; 3Shape A/S, CEREC Primescan; Dentsply Sirona, i700; Medit, Aoralscan3; Shining 3D, and iTero Element 5D Plus; Align Technologies). The null hypotheses were that no difference would be found in the trueness and precision of the complete arch implant

scans recorded with the different scanning techniques tested and recorded using the IOSs assessed.

MATERIAL AND METHODS

A maxillary edentulous stone cast with 6 implant abutment analogs (MultiUnit Abutment Plus Replica; Nobel Biocare) was obtained. The implant abutment analogs were located at the right and left lateral incisors, right and left first premolars, and right and left first molars.

Five groups were developed based on the IOS tested: TRIOS 5 (TRIOS 5, v.24.1.7; 3Shape A/S), Primescan (CEREC Primescan, Connect v.5.2.7; Dentsply Sirona), i700 (i700, Medit scan for clinics v.1.12.2, Medit link v.3.3.2; Medit), Aoralscan3 (Aoralscan3, v.1.0.0.3115; Shining 3D), and iTero (iTero Element 5D Plus, v.2.8.25.70; Align Technologies). Except for the TRIOS 5 and iTero devices, all the remaining IOS systems assessed were calibrated before data collection and every 10 scans by using the corresponding calibration device and following the manufacturer's protocol.²⁸ All the experimental scans were recorded under 1000-lux ambient illumination conditions (LX1330B Light Meter; Dr. Meter Digital Illuminance).^{29–31} The scanning distance recommended by each IOS manufacturer was followed (0 mm for TRIOS 5 and iTero, 2 mm for Primescan, and between 4 to 6 mm for Aoralscan3).³² Experimental scans were recorded without rescanning procedures.^{33,34} In the i700 system, a 23-mm focal length was chosen. Additionally, the smart stitching, color, and scan filtering functions were disabled, but the reliability function was activated. All the experimental scans were obtained by a prosthodontist (M.R.-L.) with 11-years of experience with IOSs.^{35,36}

Two subgroups were created depending on the implant scanning technique used to record the complete arch implant scans: a nonsplinted (NS-ISB subgroup) or noncalibrated splinting (NCS-IOC group) implant scanning technique ($n=10$). The order of the IOSs for each subgroup was randomized by using a deck of cards.

A new ISB (TrueScan Body for MUA Abutment Nobel Biocare RP; TruAbutment) was hand tightened on each implant abutment of the maxillary reference stone cast according to the manufacturer recommendations. The ISBs were maintained in the same position until all the specimens of the NS-ISB subgroup had been obtained. Additionally, a reference scan was obtained by using a calibrated laboratory scanner (T710; Medit) according to the scanning protocol recommended by the manufacturer. The reference scan was exported in a standard tessellation language (STL) file format.

For the specimen acquisition of the TRIOS 5-NS-ISB, Primescan-NS-ISB, i700-NS-ISB, Aoralscan3-NS-ISB, and iTero-NS-ISB subgroups, consecutive complete arch

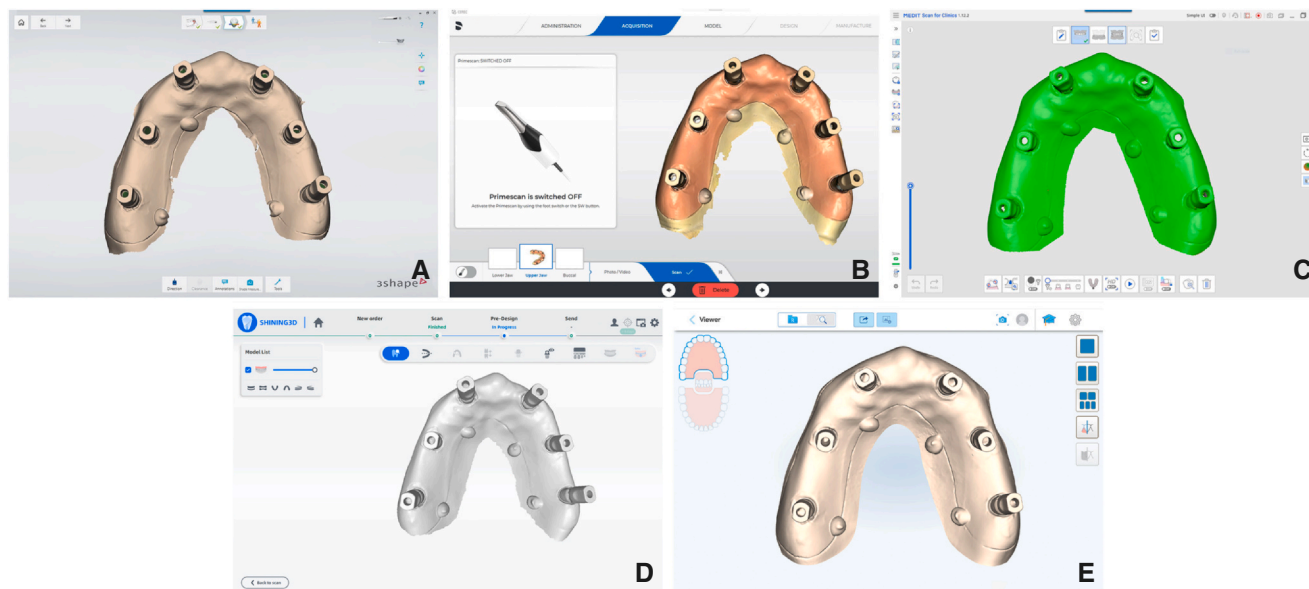


Figure 1. Representative specimens NS-ISB subgroup. A, TRIOS 5-NS-ISB subgroup. B, Primescan-NS-ISB subgroup. C, i700-NS-ISB subgroup. D, Aoralscan3-NS-ISB subgroup. E, iTero-NS-ISB subgroup.

implant scans were obtained following a circumferential scanning pattern using the corresponding IOS.³⁷ The scan started in the ISB located in the right first molar and continued towards the contralateral ISB with a circumferential motion around each ISB. Each scan was automatically postprocessed by the IOS software program (Fig. 1). The experimental scans were exported in an STL file format. Afterwards, the ISBs were retrieved from the reference stone cast.

For the specimen recording of the TRIOS 5-NCS-IOC, Primescan-NCS-IOC, i700-NCS-IOC, Aoralscan3-NCS-IOC, and iTero-NCS-IOC subgroups, a horizontal ISB (IOConnect; TruAbutment) was hand tightened on each implant abutment of the reference cast. The horizontal ISBs need to connect in the center of the palate. Three sizes (S, M, and L) of the horizontal ISBs were available, aiming to facilitate connecting the horizontal ISBs in the center of the arch and avoiding their overlap (Fig. 2). A M-horizontal ISB was hand tightened in the implant abutment analogs located in the right first premolar and lateral incisor. A L-horizontal ISB was hand tightened in the implant abutment analog located in the right first molar and left first premolar and lateral incisor. Then, consecutive complete arch implant scans were obtained using the corresponding IOS. The intraoral scans involved the hexagon geometry of the horizontal ISBs (Fig. 3). Each scan was automatically postprocessed by the IOS software program. The experimental scans were exported in STL file format. Afterwards, the horizontal ISBs were retrieved from the reference stone cast.

Each experimental scan obtained in the NCS-IOC subgroup was imported into a computer-aided design (CAD) program (TruSuite, v.1.0.29; TruAbutment). Then, the center



Figure 2. Horizontal implant scan bodies (IOConnect; TruAbutment) with palatal orientation.

of each hexagon geometry of the horizontal ISBs contained in each experimental scan was selected, followed by the size of each horizontal ISB. The program was used to locate the geometry of the healing abutment of the system used (IOConnect AOT HS Cap FDA; TruAbutment) (Fig. 4).

A complete arch implant-supported bar was designed in the control and each experimental scan by using a dental program (DentalCAD, v.3.2. Elefsina; exocad GmbH). Each scan was imported into the CAD program. Then, the virtual implant cast was acquired by aligning the ISBs of the digital scan and the CAD file of the ISB chosen. Subsequently, a complete arch implant-supported bar was designed by using the tools of the CAD program (Fig. 5). Lastly, the bar designs were imported into a metrology program (Geomagic; 3D Systems), and linear and angular measurements among the implants of

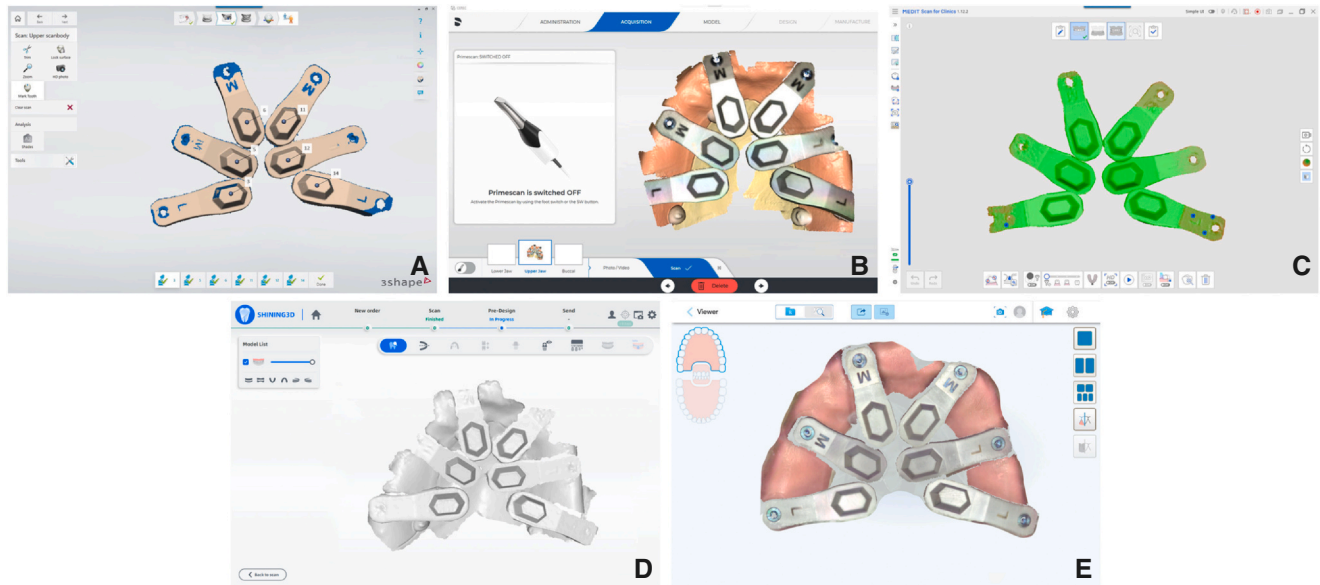


Figure 3. Representative specimens NCS-IOC subgroup. A, TRIOS 5- NCS-IOC subgroup. B, Primescan-NCS-IOC subgroup. C, i700-NCS-IOC subgroup. D, Aoralscan3-NCS-IOC subgroup. E, iTero-NCS-IOC subgroup.

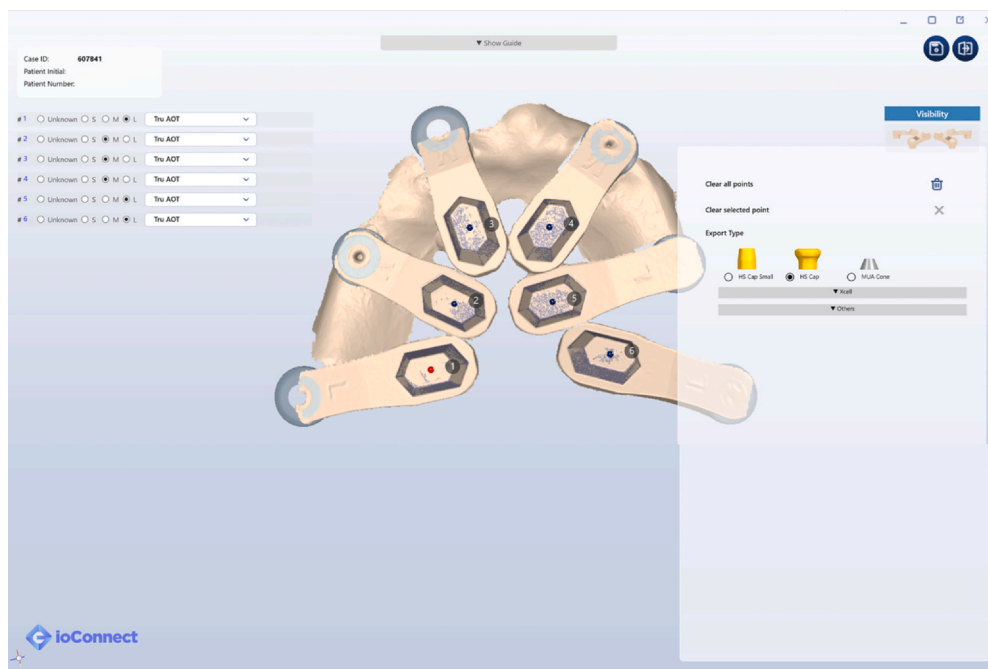


Figure 4. Representative procedures performed in NCS-IOC subgroups by using specific program (TruSuite, v.1.0.29; TruAbutment).

each bar design were obtained. The z-plane was located at the apical base of each implant interface, followed by the longitudinal axis of each implant. The point located at the intersection between the z-plane and the longitudinal axis of the implant abutment was used to measure the Euclidean linear distances among the 6 implant abutments. Additionally, the longitudinal axes of the implant abutments were used to calculate the Euclidean angular distances among the implants.

Trueness was described as the average linear and angular measurements between the reference and experimental scans.³⁸ Precision was described as the measurement variations for each group.³⁸ The Q-Q plots indicated the normality of residuals in regression models, while the variance across the groups was significantly unequal. Therefore, the 2-way ANOVA Welch test followed by the post hoc pairwise multiple comparison Tukey test was used to analyze trueness ($\alpha=.05$).

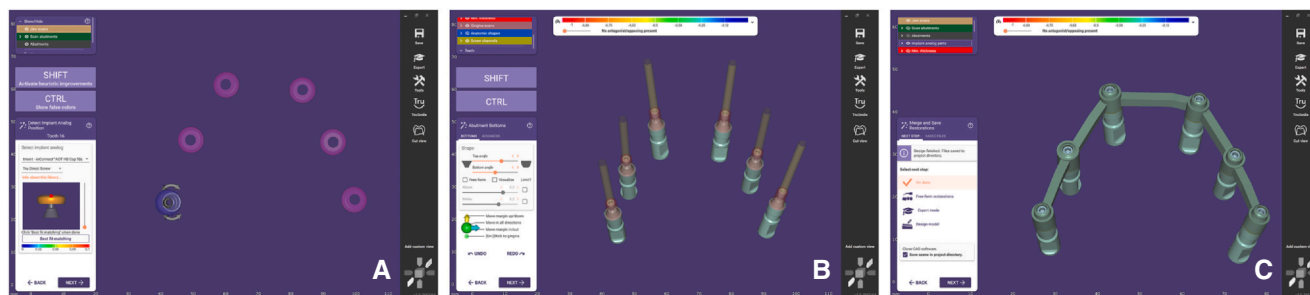


Figure 5. Representative procedures for designing implant-supported bars on each specimen. A, Alignment of CAD file and same geometry of experimental scan. B, Implant abutment analogs. C, Implant-supported bar designed on implant abutment analogs.

Table 1. Overall linear and angular measurement discrepancies measured among groups tested

Group	Subgroup	Overall Mean ±SD Linear Discrepancies (μm)	Overall Mean ±SD Angular Discrepancies (Degrees)
TRIOS5	NCS-IOC	30 ±5	0.39 ±0.09
	NS-ISB	70 ±22	0.43 ±0.09
Primescan	NCS-IOC	26 ±8	0.34 ±0.12
	NS-ISB	78 ±28	0.62 ±0.15
i700	NCS-IOC	41 ±19	0.31 ±0.10
	NS-ISB	195 ±161	0.40 ±0.15
Aoralscan3	NCS-IOC	34 ±10	0.29 ±0.13
	NS-ISB	72 ±24	0.29 ±0.06
iTero	NCS-IOC	58 ±17	0.25 ±0.07
	NS-ISB	87 ±33	0.63 ±0.13

IOC, IOConnect; ISB, implant scan body; NCS, noncalibrated splinted; NS, nonsplinted; SD, standard deviation.

The Levene test followed by pairwise multiple comparison using the Wilcoxon rank sum test with continuity correction data was used to analyze precision ($\alpha=.05$). Data were analyzed using a statistical program (SAS, v.3.81, Enterprise Edition; SAS Institute Inc).

RESULTS

The discrepancies measured among the subgroups tested are presented in Table 1. Regarding the linear measurement discrepancies, the 2-way ANOVA test revealed significant linear trueness discrepancies among the groups ($df=1$, $MS=0.09679$, $F=32.67$, $P<.001$) and subgroups ($df=4$, $MS=0.01652$, $F=5.58$, $P<.001$), with a significant interaction group×subgroup ($df=4$, $MS=0.01328$, $F=4.48$, $P=.002$) (Fig. 6A). Regarding group (scanning technique) effect, the Tukey test demonstrated significant linear trueness discrepancies among the groups. The NCS-IOC group obtained significantly better linear trueness than the NS-ISB group (Fig. 6B). Regarding subgroup (IOS system) effect, the Tukey test demonstrated significant linear trueness discrepancies among the subgroups tested (Table 2). The TRIOS5 (mean of 50 μm) and i700 (mean of 118 μm) ($P=.002$), Primescan (mean of 52 μm) and i700 ($P=.002$), and i700 and Aoralscan3 (mean of 53 μm) ($P=.003$) were

significantly different from each other. Therefore, the TRIOS5, Primescan, and Aoralscan3 systems obtained significantly better linear trueness than the i700 device (Fig. 6C, D). Additionally, the Levene test revealed significant linear precision discrepancies among the groups tested ($P=.003$). The NCS-IOC group (mean of 38 μm) obtained significantly better linear precision than the NS-ISB group (mean of 100 μm).

Regarding the angular measurement discrepancies, the 2-way ANOVA test revealed significant angular trueness discrepancies among the groups ($df=1$, $MS=0.6209$, $F=47.81$, $P<.001$) and subgroups ($df=4$, $MS=0.1142$, $F=8.79$, $P<.001$), with a significant interaction group×subgroup ($df=4$, $MS=0.1410$, $F=10.86$, $P<.001$) (Fig. 6E). Regarding the group (scanning technique) effect, the Tukey test demonstrated significant angular trueness discrepancies among the groups. The NCS-IOC group (mean of 0.32 degrees) obtained significantly better angular trueness than the NS-ISB group (mean of 0.47 degrees) (Fig. 6F). Regarding subgroup (IOS system) effect, the Tukey test demonstrated significant angular trueness discrepancies among the subgroups tested (Table 3). The TRIOS 5 (mean of 0.41 degrees) and Aoralscan3 (mean of 0.29 degrees) ($P=.008$), Primescan (mean of 0.48 degrees) and i700 (mean of 0.35 degrees) ($P=.005$), Primescan and Aoralscan3 ($P<.001$), and Aoralscan3 and iTero (mean of 0.44 degrees) ($P<.001$) were significantly different from each other. Therefore, the i700 and Aoralscan3 systems obtained the best angular trueness (Fig. 6G, H). Additionally, the Levene test revealed significant angular precision discrepancies among the groups tested ($P<.001$). The NCS-IOC group (mean of 0.017 degrees) had significantly better angular precision than the NS-ISB group (mean of 0.087 degrees). Moreover, the Levene test had significant angular precision discrepancies among the subgroups tested ($P<.001$). The TRIOS 5 and Aoralscan3 obtained the best angular precision ($P<.001$).

DISCUSSION

The results of this in vitro investigation revealed that the implant scanning technique used and IOS selected

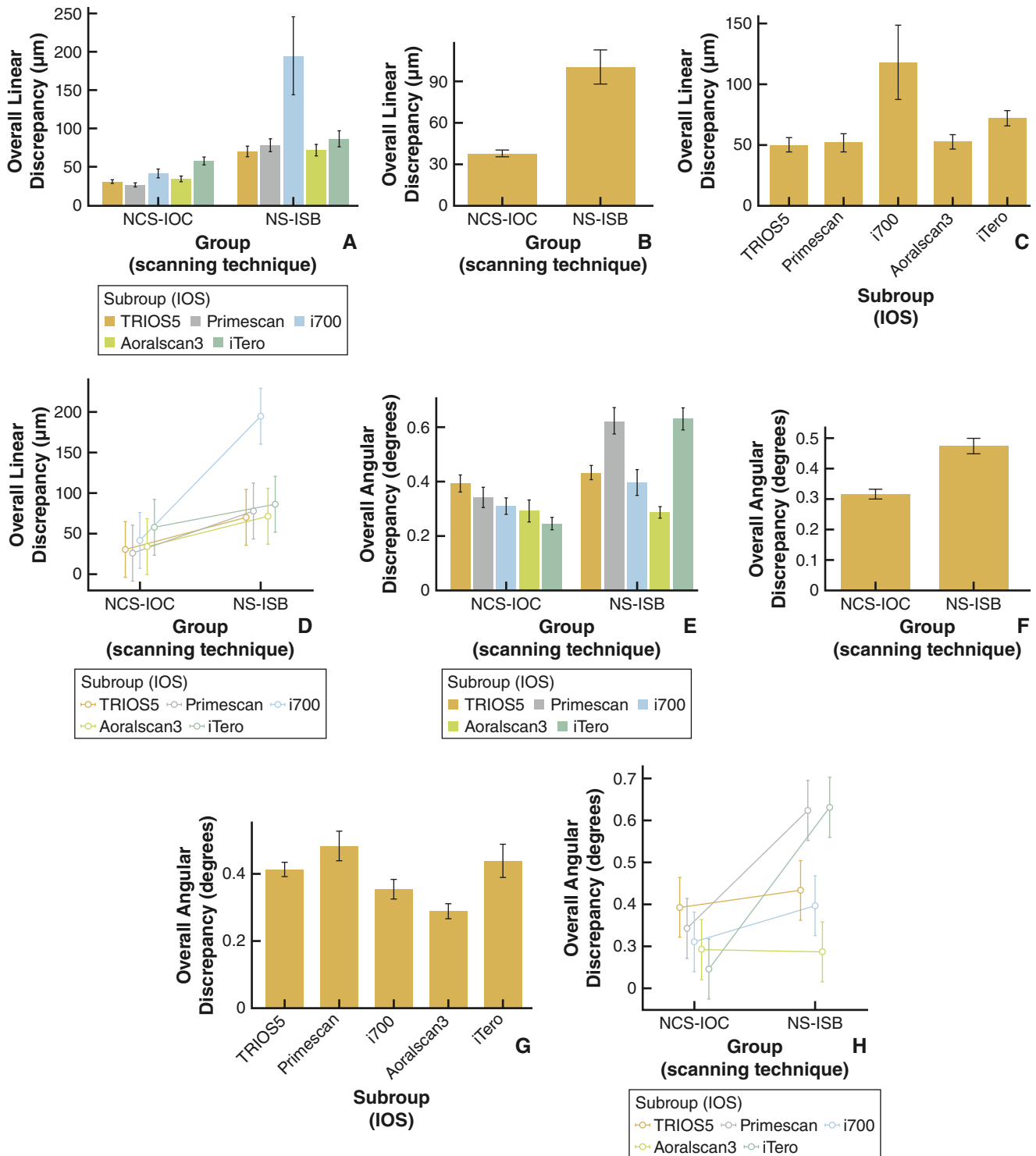


Figure 6. A, Boxplot of linear measurements measured among subgroups tested. B, Plot overall linear measurement measured among groups tested. C, Plot overall linear measurement measured among subgroups tested. D, Group \times Subgroup interaction plot. E, Boxplot of angular measurements measured among subgroups tested. F, Plot overall angular measurement measured among groups tested. G, Plot overall angular measurement measured among subgroups tested. H, Group \times Subgroup interaction plot. IOC, IOConnect; IOS, intraoral scanner; ISB, implant scan body; NCS, noncalibrated splinting; NS, nonsplinting.

Table 2. Post hoc overall linear discrepancies comparisons – subgroup (IOS system)

Subgroup Comparison		Mean Difference	SE	df	t	Ptukey
TRIOS 5	Primescan	−0.00189	0.0172	90.0	−0.1097	>.999
	i700	−0.06772	0.0172	90.0	−3.9341	.002*
	Aoralscan3	−0.00258	0.0172	90.0	−0.1501	>.999
	iTero	−0.02183	0.0172	90.0	−1.2684	.711
Primescan	i700	−0.06583	0.0172	90.0	−3.8244	.002*
	Aoralscan3	−6.94e−4	0.0172	90.0	−0.0403	>.999
	iTero	−0.01994	0.0172	90.0	−1.1586	.775
	Aoralscan3	0.06513	0.0172	90.0	3.7840	.003*
i700	Aoralscan3	0.04588	0.0172	90.0	2.6657	.067
	iTero	−0.01925	0.0172	90.0	−1.1183	.796

Comparisons based on estimated marginal means

*Subgroups significantly different ($P<.05$)

Table 3. Post hoc overall angular discrepancies comparisons – subgroup (IOS system)

Subgroup Comparison		Mean Difference	SE	df	t	Ptukey
TRIOS 5	Primescan	−0.0697	0.0360	90.0	−1.935	.307
	i700	0.0596	0.0360	90.0	1.653	.468
	Aoralscan3	0.1238	0.0360	90.0	3.436	.008*
	iTero	−0.0255	0.0360	90.0	−0.708	.954
Primescan	i700	0.1293	0.0360	90.0	3.588	.005*
	Aoralscan3	0.1935	0.0360	90.0	5.371	<.001*
	iTero	0.0442	0.0360	90.0	1.227	.736
	Aoralscan3	0.0642	0.0360	90.0	1.783	.390
i700	iTero	−0.0851	0.0360	90.0	−2.361	.136
	Aoralscan3	−0.1493	0.0360	90.0	−4.144	<.001*

Comparisons based on estimated marginal means

*Subgroups significantly different ($P<.05$)

impacted the trueness and precision of complete arch implant scans. The noncalibrated splinting implant scanning technique with a palatal orientation demonstrated better accuracy outcomes when compared with the standard ISBs or nonsplinting method tested. Therefore, the null hypothesis that no difference would be found in the trueness and precision of the complete arch implant scans recorded with the different scanning techniques tested and recorded using the IOSs assessed was rejected.

Nonsplinting implant scanning methods have been reported to have a trueness ranging from 41 to 303 μm and a mean precision value varying from 25 to 181 μm .^{1–15} In comparison, noncalibrated splinting implant scanning methods have a trueness ranging from 49 to 240 μm and a mean precision value varying from 45 to 176 μm .^{1,12} However, multiple noncalibrated splinting designs in which the ISBs were connected following the dental arch shape have been described.^{1,12} The authors are unaware of a previous investigation that analyzed the accuracy of the selected noncalibrated splinting implant scanning technique with a palatal orientation (IOConnect; TruAbutment). Therefore, direct comparisons with previously published studies are not feasible. However, while different noncalibrated splinting implant scanning methods have been described in the dental literature, this is a unique system with a different orientation of the ISBs, being connected in the center of the arch. Therefore, comparisons with other noncalibrated splinting implant scanning techniques may be inappropriate. However, in the present investigation, the

noncalibrated implant scanning technique tested demonstrated significantly better linear and angular trueness and precision mean values than the nonsplinting method considered. The noncalibrated splinting implant scanning technique showed an overall linear discrepancy ranging from $26 \pm 8 \mu\text{m}$ to $58 \pm 17 \mu\text{m}$ and an overall angular discrepancy ranging from 0.25 ± 0.07 degrees to 0.39 ± 0.09 degrees. The noncalibrated splinting implant scanning technique obtained accuracy values that could be considered within the clinically acceptable discrepancy. The nonsplinting implant scanning technique showed an overall linear discrepancy ranging from $72 \pm 24 \mu\text{m}$ to $195 \pm 161 \mu\text{m}$ and an overall angular discrepancy ranging from 0.29 ± 0.06 degrees to 0.63 ± 0.13 degrees. Therefore, the nonsplinting implant scanning technique may not provide a clinically acceptable scanning method.

The noncalibrated splinting with palatal orientation method facilitated the digitizing method, as it only required the scanning of the hexagon geometry of the horizontal scan body which is oriented in the center of the arch. Additionally, as the horizontal ISBs were connected in the center of the arch, the scanning procedure does not involve scanning the entire arch, minimizing the scanning time and number of photographs. The scanning performance varied among the different IOS systems, and scanning nonsplinting ISBs is more challenging for one IOS when compared with others. However, the present investigation did not analyze the scanning time or number of photographs discrepancies among the 2 techniques tested. Laboratory

and clinical studies are needed to further evaluate scanning accuracy and scanning time among the different implant scanning techniques described.¹

The IOS system and version have been reported to impact the accuracy of digital implant scans.^{7,11,39,40} Comparisons with previous studies are challenging because of different research methodology; however, the results of the present investigation were consistent with this finding. Trueness and precision discrepancies in the linear and angular measurements were found among the complete arch implant scans recorded by using the IOSs tested. Furthermore, the TRIOS 5, Primescan, and Aoralscan3 systems obtained better linear trueness than the i700 device, while the i700 and Aoralscan3 systems demonstrated the best angular trueness. The TRIOS5 and Aoralscan3 obtained the best angular precision.

Limitations of the present study included the in vitro conditions, limited implant designs, positions, inter-implant distances, and the standard implant scan body design tested. Furthermore, an extraoral scanner was selected to obtain the reference scan. Studies are required to further evaluate the accuracy of the different implant scanning techniques for recording the definitive virtual implant casts, as well as to analyze the impact of the IOS system and version on the accuracy of implant scans.

CONCLUSIONS

Based on the results of this in vitro study, the following conclusions were drawn:

1. The implant scanning technique and IOSs tested impacted the scanning trueness and precision of the complete arch implant scans.
2. The non calibrated implant scanning technique (IOConnect; TruAbutment) had significantly better accuracy (trueness and precision) outcomes (linear and angular discrepancies) when compared with the nonsplinting implant scanning method considered (standard nonsplinted implant scan bodies).
3. The noncalibrated splinting implant scanning technique showed an overall linear discrepancy ranging from $26 \pm 8 \mu\text{m}$ to $58 \pm 17 \mu\text{m}$ and overall angular discrepancy ranging from 0.25 ± 0.07 degrees to 0.39 ± 0.09 degrees. The noncalibrated splinting implant scanning technique obtained accuracy values that could be considered within the clinically acceptable discrepancy range.
4. The nonsplinting implant scanning technique showed an overall linear discrepancy ranging from $72 \pm 24 \mu\text{m}$ to $195 \pm 161 \mu\text{m}$ and overall angular discrepancy ranging from 0.29 ± 0.06 degrees to 0.63 ± 0.13 degrees. Therefore, the nonsplinting

implant scanning technique may not provide a clinically acceptable scanning method.

5. The TRIOS 5, Primescan, and Aoralscan3 systems had significantly better linear trueness than the i700 device, while the i700 and Aoralscan3 systems demonstrated the best angular trueness. The TRIOS 5 and Aoralscan3 had the best angular precision.

REFERENCES

1. Revilla-León M, Gómez-Polo M, Rutkunas V, et al. Classification of complete-arch implant scanning techniques recorded by using intraoral scanners. *J Esthet Restor Dent* 2024.
2. Vitai V, Németh A, Sólyom E, et al. Evaluation of the accuracy of intraoral scanners for complete-arch scanning: A systematic review and network meta-analysis. *J Dent*. 2023;137:104636.
3. Papaspyridakos P, De Souza A, Finkelman M, et al. Digital vs conventional full-arch implant impressions: A retrospective analysis of 36 edentulous jaws. *J Prosthodont*. 2023;32:325–330.
4. Wu HK, Wang J, Chen G, et al. Effect of novel prefabricated auxiliary devices attaching to scan bodies on the accuracy of intraoral scanning of complete-arch with multiple implants: An in-vitro study. *J Dent*. 2023;138:104702.
5. Albánchez-González MI, Brinkmann JC, Peláez-Rico J, et al. Accuracy of digital dental implants impression taking with intraoral scanners compared with conventional impression techniques: A systematic review of in vitro studies. *Int J Environ Res Public Health*. 2022;19:2026.
6. Ren S, Jiang X, Lin Y, Di P. Crown accuracy and time efficiency of cement-retained implant-supported restorations in a complete digital workflow: A randomized control trial. *J Prosthodont*. 2022;31:405–411.
7. Schmidt A, Wöstmann B, Schlenz MA. Accuracy of digital implant impressions in clinical studies: A systematic review. *Clin Oral Implants Res*. 2022;33:573–585.
8. Rutkunas V, Bilis V, Simonaitis T, et al. The effect of different implant impression splinting techniques and time on the dimensional accuracy: An in vitro study. *J Dent*. 2022;126:104267.
9. Kernen FR, Recca M, Vach K, et al. In vitro scanning accuracy using different aids for multiple implants in the edentulous arch. *Clin Oral Implants Res*. 2022;33:1010–1020.
10. Wulfman C, Naveau A, Rignon-Bret C. Digital scanning for complete-arch implant-supported restorations: A systematic review. *J Prosthet Dent*. 2020;124:161–167.
11. Mangano FG, Hauschild U, Veronesi G, et al. Trueness and precision of 5 intraoral scanners in the impressions of single and multiple implants: A comparative in vitro study. *BMC Oral Health*. 2019;19:101.
12. Paratelli A, Vania S, Gómez-Polo C, et al. Techniques to improve the accuracy of complete arch implant intraoral digital scans: A systematic review. *J Prosthet Dent*. 2023;129:844–854.
13. Ma J, Zhang B, Song H, et al. Accuracy of digital implant impressions obtained using intraoral scanners: A systematic review and meta-analysis of in vivo studies. *Int J Implant Dent*. 2023;9:48.
14. Flügge T, van der Meer WJ, Gonzalez BG, et al. The accuracy of different dental impression techniques for implant-supported restorations: A systematic review and meta-analysis. *Clin Oral Implants Res*. 2018;29:374–392.
15. Wulfman C, Naveau A, Rignon-Bret C. Digital scanning for complete-arch implant-supported restorations: A systematic review. *J Prosthet Dent*. 2020;124:161–167.
16. Önöröl Ö, Kurtulmus-Yilmaz S, Toksoy D, Ozan O. Effect of angulation on the 3D trueness of conventional and digital implant impressions for multi-unit restorations. *J Adv Prosthodont*. 2023;15:290–301.
17. Sequeira V, Harper MT, Lilly CL, Bryington MS. Accuracy of digital impressions at varying implant depths: An in vitro study. *J Prosthodont*. 2023;32:54–61.
18. Carneiro Pereira AL, Medeiros VR, Da Fonte Porto Carneiro A. Influence of implant position on the accuracy of intraoral scanning in fully edentulous arches: A systematic review. *J Prosthet Dent*. 2021;126:749–755.
19. Laohverapanich K, Luangchana P, Anunmana C, Pornprasertsuk-Damrongsri S. Different implant subgingival depth affects the trueness and precision of the 3D dental implant position: A comparative in vitro study among five digital scanners and a conventional technique. *Int J Oral Maxillofac Implants*. 2021;36:1111–1120.
20. Thanasisuebwong P, Kulchotirat T, Anunmana C. Effects of inter-implant distance on the accuracy of intraoral scanner: An in vitro study. *J Adv Prosthodont*. 2021;13:107–116.
21. Tan M, Yee S, Wong K, et al. Comparison of three-dimensional accuracy of digital and conventional implant impressions: Effect of interimplant distance in an edentulous arch. *Int J Oral Maxillofac Implants*. 2019;34:366–380.

22. Gómez-Polo M, Donmez MB, Çakmak G, et al. Influence of implant scan body design (height, diameter, geometry, material, and retention system) on intraoral scanning accuracy: A systematic review. *J Prosthodont*. 2023;32:165–180.
23. Tan JZH, Tan MY, See Toh YL, et al. Three- dimensional positional accuracy of intraoral and laboratory implant scan bodies. *J Prosthet Dent*. 2022;128:735–744.
24. Gómez-Polo M, Álvarez F, Ortega R, et al. Influence of the implant scan body bevel location, implant angulation and position on intraoral scanning accuracy: An in vitro study. *J Dent*. 2022;121:104122.
25. Revilla-León M, Kois DE, Kois JC. A guide for maximizing the accuracy of intraoral digital scans. Part 1: Operator factors. *J Esthet Restor Dent*. 2023;35:230–240.
26. Revilla-León M, Kois DE, Kois JC. A guide for maximizing the accuracy of intraoral digital scans: Part 2-Patient factors. *J Esthet Restor Dent*. 2023;35:241–249.
27. Revilla-León M, Lanis A, Yilmaz B, et al. Intraoral digital implant scans: Parameters to improve accuracy. *J Prosthodont*. 2023;32:150–164.
28. Revilla-León M, Gohil A, Barmak AB, et al. Influence of ambient temperature changes on intraoral scanning accuracy. *J Prosthet Dent*. 2023;130:755–760.
29. Revilla-León M, Jiang P, Sadeghpour M, et al. Intraoral digital scans-Part 1: Influence of ambient scanning light conditions on the accuracy (trueness and precision) of different intraoral scanners. *J Prosthet Dent*. 2020;124:372–378.
30. Revilla-León M, Subramanian SG, Özcan M, Krishnamurthy VR. Clinical study of the influence of ambient light scanning conditions on the accuracy (trueness and precision) of an intraoral scanner. *J Prosthodont*. 2020;29:107–113.
31. Revilla-León M, Subramanian SG, Att W, Krishnamurthy VR. Analysis of different illuminance of the room lighting condition on the accuracy (trueness and precision) of an intraoral scanner. *J Prosthodont*. 2021;30:157–162.
32. Button H, Kois JC, Barmak AB, et al. Scanning accuracy and scanning area discrepancies of intraoral digital scans acquired at varying scanning distances and angulations among 4 different intraoral scanners. *J Prosthet Dent*. 2024;132:1044–1060.
33. Revilla-León M, Quesada-Olmo N, Gómez-Polo M, et al. Influence of rescanning mesh holes on the accuracy of an intraoral scanner: An in vivo study. *J Dent*. 2021;115:103851.
34. Revilla-León M, Sicilia E, Agustín-Panadero R, et al. Clinical evaluation of the effects of cutting off, overlapping, and rescanning procedures on intraoral scanning accuracy. *J Prosthet Dent*. 2023;130:746–754.
35. Kim J, Park JM, Kim M, et al. Comparison of experience curves between two 3-dimensional intraoral scanners. *J Prosthet Dent*. 2016;116:221–230.
36. Lim JH, Park JM, Kim M, et al. Comparison of digital intraoral scanner reproducibility and image trueness considering repetitive experience. *J Prosthet Dent*. 2018;119:225–232.
37. Gómez-Polo M, Cascos R, Ortega R, et al. Influence of scanning pattern on accuracy, time, and number of photographs of complete-arch implant scans: A clinical study. *J Dent*. 2024;150:105310.
38. International Organization for Standardization. ISO 5725–1:1994. Accuracy (trueness and precision) of measurement methods and results - Part 1: General principles and definitions. (<https://www.iso.org/obp/ui/#iso:std:iso:5725:-1:ed-1:v1:en>) Accessed 02–01–20.
39. Revell G, Simon B, Mennito A, et al. Evaluation of complete-arch implant scanning with 5 different intraoral scanners in terms of trueness and operator experience. *J Prosthet Dent*. 2022;128:632–638.
40. Revilla-León M, Barmak AB, Lanis A, Kois JC. Influence of connected and nonconnected calibrated frameworks on the accuracy of complete arch implant scans obtained by using four intraoral scanners, a desktop scanner, and a photogrammetry system. *J Prosthet Dent* 2024.

Corresponding author:

Dr Marta Revilla-León
Kois Center
1001 Fairview Avenue North, # 2200
Seattle, WA 98109
Email: marta.revilla.leon@gmail.com

Copyright © 2025 by the Editorial Council of *The Journal of Prosthetic Dentistry*. All rights are reserved, including those for text and data mining, AI training, and similar technologies.
<https://doi.org/10.1016/j.prosdent.2025.02.020>